Proceedings of the EuroGNC 2013, 2nd CEAS Specialist Conference on
Guidance, Navigation & Control, Delft University of Technology, Delft,
The Netherlands, April 10-12, 2013

Design of a Waypoint Tracking Control Algorithm for Parachute-Payload Systems

Gonenc Gursoy, Anna Prach, Ilkay Yavrucuk

Abstract This paper describes the development of an automatic control algorithm and a waypoint navigation approach for a parachute-payload system. A model is developed and the effectiveness of the controller architecture using classical control methods and waypoint navigation are demonstrated. Simulation results show that an introduced waypoint update criteria for the heading reference allows to obtain sufficient waypoint tracking. Simulation results are performed under varying wind conditions.

1 Introduction

The use of parachutes is known to be one of the cost-effective methods for delivering payloads of various weights and sizes to a desired locations. Guidance algorithms for parachute-payload systems are sensitive to flight conditions and especially to atmospheric disturbance. The guidance law architecture effects the ability of a parachute to reach a target destination. A proper implementation is necessary to ensure that a payload is delivered within a close range around a target location, which in the case of adverse weather conditions becomes a challenging task to perform.

A number of studies that concern the development of autonomous guidance, navigation and control (GNC) algorithms for parachute-payload systems are available in literature. In [1], for example, a GNC algorithm for an autonomous parafoil sys-

Gonenc Gursoy
Middle East Technical University, Ankara, Turkey, e-mail: gonenc.gursoy@metu.edu.tr

Anna Prach
Middle East Technical University, Ankara, Turkey, e-mail: anna.prach@metu.edu.tr

Dr. Ilkay Yavrucuk
Asst. Professor at Middle East Technical University, Department of Aerospace Engineering, Ankara, Turkey, e-mail: yavrucuk@metu.edu.tr

tem is developed, where the waypoints are distributed along a 'T'-formed pattern. In [2] the so-called planar Dubins path synthesis is implemented, where an altitude margin parameter is defined and used by the guidance algorithm to quantitatively compare initial conditions and determine the reachability of the specified final configuration. Kaminer and Yakimenko [3] developed a real-time trajectory generation algorithm that consists of three segments, which are fused according to the navigation law. Reference [4] reports a two and three dimensional waypoint tracking algorithm introducing waypoint altitude constraints in addition to the horizontal position constraints.

A majority of previous controller research for parachute-payload implementations have revolved around the development of nonlinear controllers and optimal tracking controllers. For example, in [2] a non-linear tracking control algorithm is applied to the parafoil model to track the generated reference trajectories with a capability to reconfigure these trajectories onboard whenever necessary. In [3] a nonlinear controller is developed to track the reference trajectory. The controller uses only the GPS position and velocity measurements, which satisfied the low cost onboard avionics requirements. Reference [4] introduces an adaptive stability augmentation system design.

A model predictive control strategy for parafoil-payload systems is presented in [5] and [7]. Reference [5] introduced a modified version of a standard model predictive control strategy that accounts for a so-called brake deflection bias, and its implementation is presented for the parafoil with an aircraft being a payload. In [7] the control algorithm combines a state-dependent Riccati equation with a nonlinear model. In [6] an LQ-Servo optimal controller is designed to provide adequate tracking of a prescribed gliding path that is expressed in terms of a desired airspeed and a flight path angle.

In [1] an implementation of a classic control algorithm is proposed. The developed approach enables the system to determine a pre-defined landing point with a reasonable accuracy even in presence of turbulence, wind, inaccuracies in system parameters and sensor errors.

The aspects of modeling of parachute-payload systems are covered in various sources. In [5], [7] a reduced-order 6-DOF parafoil and payload system model is introduced. A high fidelity nonlinear 8-DOF model is utilized in [11]. The development of 9-DOF models are reported in [6], [8] - [10].

This paper focuses on the use of the waypoint update criteria and its implementation to waypoint tracking with classic controllers for a parachute-payload system. For the navigation and control problem, a nonlinear 9-DOF parachute-payload model is developed. Two different control strategies for a heading controller with proportional and a PID control are used. It is assumed that heading, position and velocity measurements are available. Different scenarios, including cases of varying wind conditions are applied in simulation.

The outline of this paper is as follows. In Sect.2 a waypoint tracking controller is presented along with a general structure of the heading controller and a waypoint update algorithm. The 9-DOF parachute-payload model is presented in Sect.3. Simulation results of the developed waypoint tracking control algorithm are presented

in Sect. 4. A comparison is made to demonstrate the difference between the two controller approaches. Finally, a varying wind is added for a more realistic and challenging simulation. Conclusions are presented in Sect. 5.

2 Waypoint Tracking Controller Design

A block diagram of the waypoint tracking controller is presented in Fig.1. A heading controller along with an outer loop controller for waypoint tracking are used. Outer loop of the control system determines the required heading reference, ψ_{ref}, for each target waypoint. The construction of the ψ_{ref} signal is based on the location of the target waypoint, $[X_{ref}\ Y_{ref}]$, and the location of the parachute, $[X_p\ Y_p]$ (seen in Fig.1). Once ψ_{ref} is established, a heading controller in the inner loop can be used to drive the parachute heading, ψ_p, to a heading reference, ψ_{ref}.

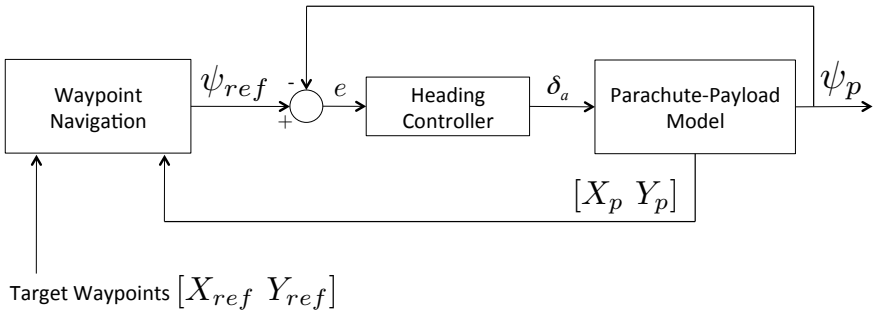

Fig. 1 A Waypoint Navigation Algorithm

The parachute location, $[X_p\ Y_p]$, and heading, ψ_p, signals are required to be measured. In real applications, it is common to use a GPS receiver to locate the system, and a magnetometer to measure the heading. It is assumed that the location, $[X_p\ Y_p]$, is known at each simulation instant, and an accurate heading measurement, ψ_p, is available.

2.1 Heading Controller

By defining a correct set of heading commands to the heading controller the system is guided to the target waypoints. In Fig.2, a departure waypoint and a target waypoint are shown along with the target heading track, ψ_t, and the track deviation angle, γ. Using a local navigation frame located at the departure point and using the known signals $[X_p\ Y_p]$ and $[X_{ref}\ Y_{ref}]$, the target heading track and track deviation

angles can be calculated from the geometry. Note, that the aim is to track the line segment between the departure and target waypoints.

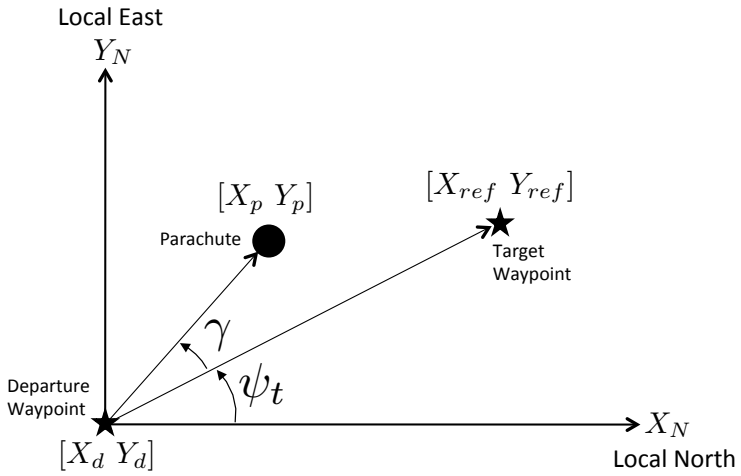

Fig. 2 Angle Definitions and Coordinate System

As a first attempt to track line segments the target heading track, ψ_t, can be used as the heading reference and the following proportional control law can be established:

$$\delta_a = K_p(\psi_t - \psi_p) \tag{1}$$

where, δ_a is the asymmetric control input of the parachute.

However, the presence of a track deviation, γ, that may appear, for example due to a gust, Eqn.(1) may not be sufficient to provide an accurate line segment tracking. Therefore, target heading track, ψ_t, must be updated with the track deviation, γ. Hence, the following update to Eqn.(1) is proposed:

$$\delta_a = K_p((\psi_t - K_\gamma\gamma) - \psi_p) \tag{2}$$

Note that in Eqn.(2), the term $(\psi_t - K_\gamma\gamma)$ is the heading reference, ψ_{ref}, and $((\psi_t - K_\gamma\gamma) - \psi_p)$ is the error term, e, as previously shown in Fig.1. Integral and derivative terms can also be added in the heading controller as shown in Fig.3.

Simulations are performed for a proportional control law given in Eqn.(2), and also for a PID controller, shown in Fig.3.

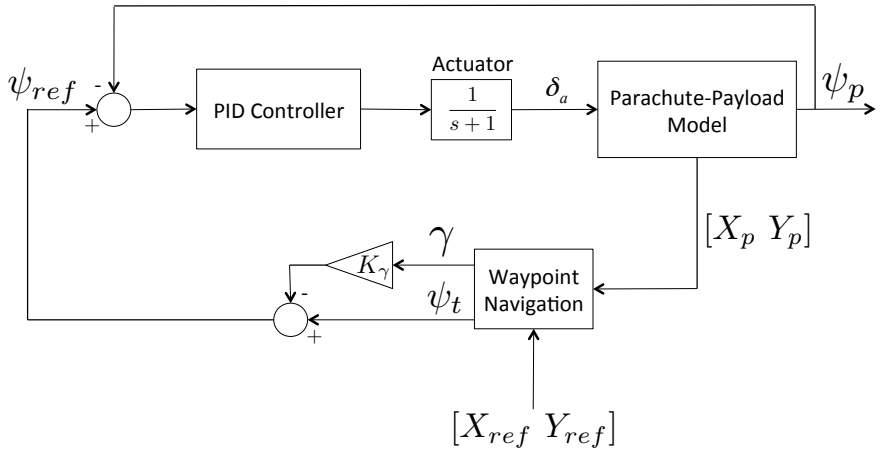

Fig. 3 Waypoint Tracking Controller Block Diagram

2.2 Waypoint Navigation

The waypoint update criteria is an essential part of a waypoint tracking controller algorithm. In general, for each target a departure point is located to begin a waypoint approach. A local navigation frame is located at each departure point and all related angles for the line segment tracking are calculated with respect to departure points as shown in Fig.2. Based on the fact that the target point is reached or missed two waypoint update criteria, namely *waypoint clearance* and *waypoint miss* conditions are established.

2.2.1 Waypoint Clearence Condition

In Fig.4, a target waypoint is aimed at the beginning. A precise pass over the area enclosed by a circle around the target indicates the clearance of the target. This criterion can be defined as the waypoint clearance condition and is satisfied when $|\vec{R}_p - \vec{R}_{ref}| < d$. Whenever a target is clear using this criterion, the next target waypoint can be aimed and a new departure point for the new target can be established. The condition for a waypoint clearance and related updates in the algorithm (at the time of clearance) are summarized below:

$$
\begin{aligned}
&if\ |\vec{R}_p - \vec{R}_{ref}| < d \\
&\quad [X_d\ Y_d]_{i+1} = [X_p\ Y_p]_i \qquad Update\ Departure\ Point \\
&\quad [X_{ref}\ Y_{ref}]_{i+1} = [X_{ref}\ Y_{ref}]_{next} \qquad Update\ Target\ Waypoint
\end{aligned}
\tag{3}
$$

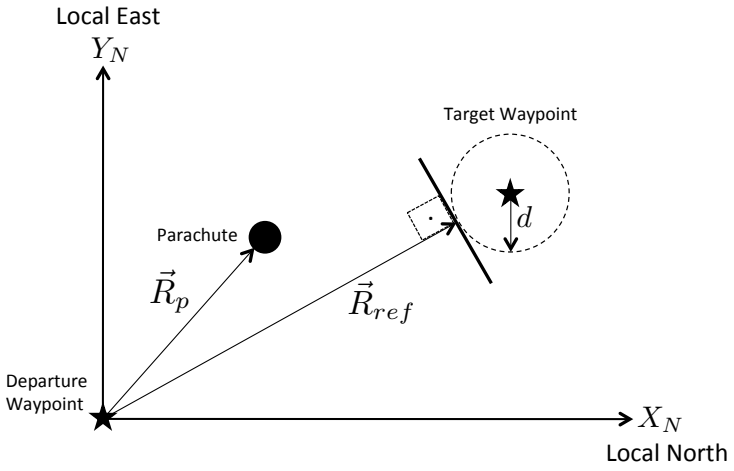

Fig. 4 Waypoint Clearance Condition

2.2.2 Waypoint Miss Condition

In the presence of a disturbance, such as a wind gust, Eqn.(3) may not be satisfied and a target can be treated as being missed. In order to establish a proper condition for a waypoint miss, a circle located at the departure point may be defined with a radius being the distance between the departure point and the target (see Fig.5). If the system moves outside of this circular region, the condition is treated as a waypoint miss. In this case, a new departure waypoint is introduced at the location where the *waypoint miss* is recorded. New departure points are established until the *waypoint clearance* condition is satisfied. The condition for missing a waypoint and related updates in the algorithm (at the time of miss) are summarized below:

$$
\begin{aligned}
&if\ |\vec{R}_p| > |\vec{R}_{dt}| && (4)\\
&\quad [X_d\ Y_d]_{i+1} = [X_p\ Y_p]_i && Update\ Departure\ Point\\
&\quad [X_{ref}\ Y_{ref}]_{i+1} = [X_{ref}\ Y_{ref}]_{current} && Do\ Not\ Update\ Target\ Waypoint
\end{aligned}
$$

For the simulations presented in this paper, Eqns.(3) and (4) are used for automatic update of target and departure waypoints whenever necessary.

3 Parachute-Payload Simulation Model

The waypoint tracking controller algorithm described in the previous section is integrated with a parachute-payload simulation model. A 9-DOF simulation model is

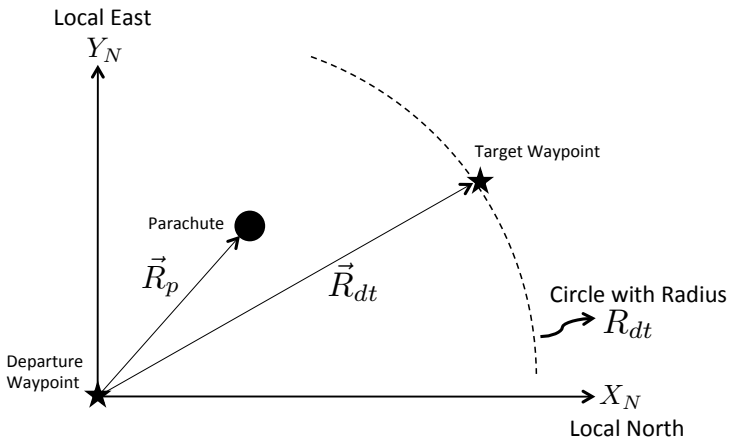

Fig. 5 Waypoint Miss Condition

developed for a parachute with a 21 m^2 wing area and 135 kg payload. The system is modeled as a rigid parafoil and a rigid payload connected at the confluence point by rigid suspension lines. Figure 6 illustrates the parachute-payload system along with the reference frames used for mathematical modeling. The payload is allowed to roll, pitch and yaw around the confluence point (point C), and is coupled to the parafoil via reaction forces and moments. All linkages are assumed to be rigid so that the distances between the centers of gravity of the parachute and the payload with respect to the point C remain constant. Geometric data used in the simulation model is given in Table 1. Similar modeling efforts can also be found in Refs. [8], [9], [10] and [11].

$$\begin{bmatrix} m_p T_{ip} & -m_p R_{cp} & 0 & T_{ip} \\ 0 & I_p & 0 & -R_{cp} T_{ip} \\ m_b T_{ib} & 0 & -m_b R_{cb} & T_{ib} \\ 0 & 0 & I_b & -R_{cb} T_{ib} \end{bmatrix} \begin{bmatrix} \dot{V}_c \\ \dot{\omega}_p \\ \dot{\omega}_b \\ F_R \end{bmatrix} = \begin{bmatrix} F^p_{aero} + W^p - m_p \Omega_p \Omega_p r_{cp} \\ M^p_{aero} - T_p T_b^T M_c - \Omega_p I_p \omega_p \\ F^b_{aero} + W^b - m_b \Omega_b \Omega_b r_{cb} \\ -\Omega_b I_b \omega_b + M_c \end{bmatrix} \tag{5}$$

Equation (5) represents a 9-DOF parachute-payload system. The state vector includes the components of the linear acceleration of the confluence point, $\dot{V}_c$, the angular acceleration components of the parachute, the payload, $\dot{\omega}_p$, $\dot{\omega}_b$, respectively, and the reaction forces, F_R, at the confluence point. The solution to Eqn.(5) can be obtained at each simulation time step. The geometric and aerodynamic data used are given in Table 1 and Table 2.

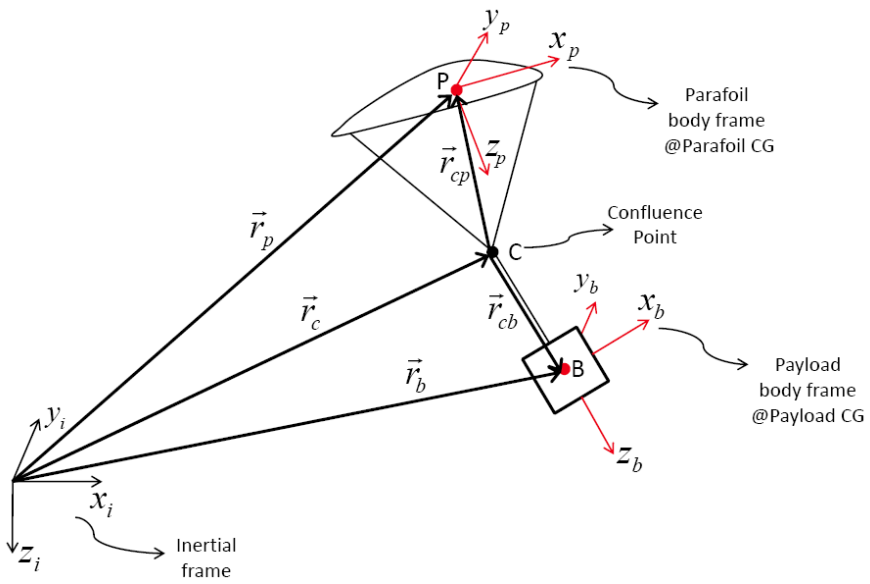

Fig. 6 Basic Parachute-Payload System

Table 1 Geometric Data for Parachute-Payload System, [8]

	Payload	Parafoil
Mass [kg]	135	13
Dimensions [m]	0.5x0.5x0.5	7x3x0.3
Surface Area [m^2]	0.5	21
Distance from joint [m]	0.5	7.5

Table 2 Aerodynamic Data for Parachute-Payload System, [8]

C_{L_0}	0.4	C_{L_α}	2.0
C_{D_0}	0.15	C_{D_α}	1.0
C_{l_p}	-0.1	C_{l_ϕ}	-0.05
C_{m_q}	-2.0	C_{m_0}	0.018
C_{n_r}	-0.07	C_{m_α}	-0.2
$C_{L_{\delta_a}}$	0.0001	$C_{L_{\delta_s}}$	0.21
$C_{D_{\delta_a}}$	0.0001	$C_{D_{\delta_s}}$	0.30
$C_{l_{\delta_a}}$	0.0021	$C_{n_{\delta_a}}$	0.004

4 Simulation Results

Three different simulation scenarios are introduced. In all simulations, the parachute is released from 3000m altitude with an average descent rate of 3.2m/s. A radius of 100m around the waypoint is chosen as the waypoint clearance condition. The system is also exposed to various wind conditions.

In the first simulation scenario a proportional controller in the inner loop is used. First, the parachute is exposed to a constant wind of 5 knots blowing in the south-north direction. As shown in Fig.7, the parachute-payload system can not precisely reach the waypoints. However, at the first and second waypoints the clearance condition is satisfied. Yet, for the third waypoint, a *waypoint miss* condition is found and a turn maneuver is performed. After the turn maneuver the fourth waypoint is reached and the parachute is driven to the target. Using the waypoint update criteria it is possible to track the waypoints even when the inner loop controller does not perform well.

The simulation concludes with performing a so-called ”eight maneuver” over the target. This is a result of the proposed algorithm, when the target waypoint is not updated for the rest of the simulation. After the fifth point, Eqns.(3) and (4) are used such that the target waypoint is kept the same. Therefore, the eight maneuver is obtained automatically.

The inner loop reference signal and the heading of the parachute is presented in Fig.8. A steady state error may be observed.

In the second simulation scenario the wind direction is changed to west-east. The same P controller as in the previous case is used for waypoint tracking. Resulting maneuveres are presented in Fig.9. For the first waypoint, the clearance condition is satisfied. However, for the second waypoint, a *waypoint miss* condition is recorded and a turn maneuver is performed as an eight maneuver. After the turn maneuver, the third waypoint is reached and the parachute is driven to the target. Note that, similar to the first scenario eight-maneuvers are obtained over the last target. In Fig.10 the inner loop error dynamics is presented.

For the third simulation scenario, the wind direction is varied from a south-north to a west-east direction. The proportional gain is kept the same as before. Simulation results along with the applied wind directions are given in Fig.11. From Fig.11 it is seen that the *waypoint miss* condition occurs two times during the simulation. After those turn maneuvers the parachute is driven to the target. The heading reference signal and the heading responses are compared in Fig.12.

Finally, the simulation scenarios described above are repeated with a PID controller as in Fig.3. Simulation results are illustrated in Figs.13-18. The performance of the inner loop is enhanced and all waypoints are tracked correctly.

The control surface deflections of the proportional controller and the PID controller applications are compared in Figs.19, 20 and 21.

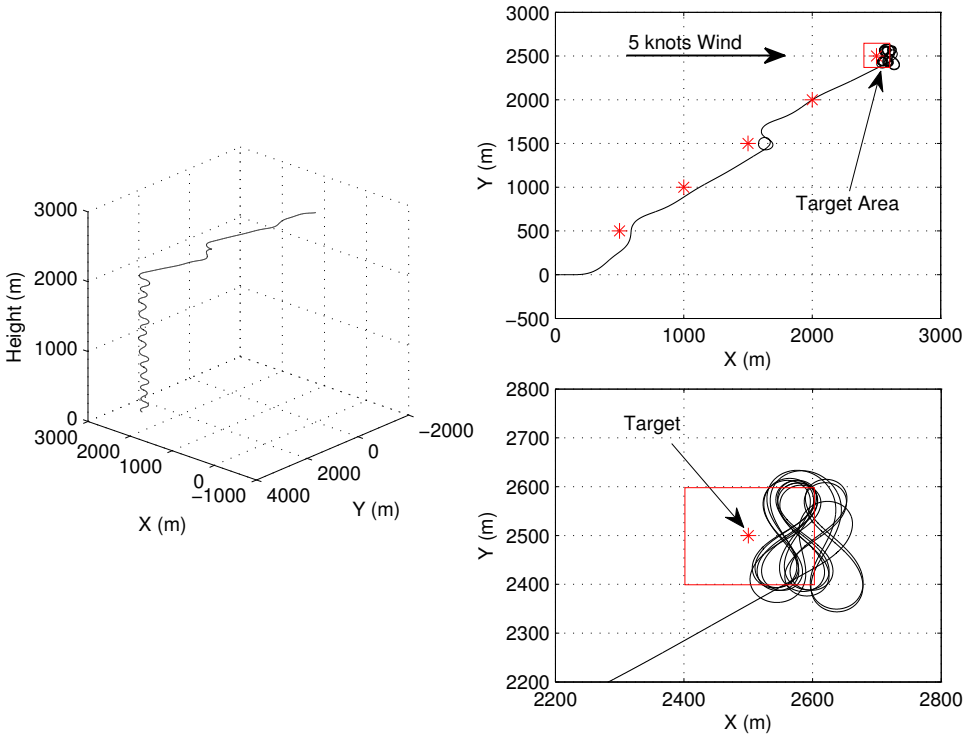

Fig. 7 Simulation-1, Proportional Control Only

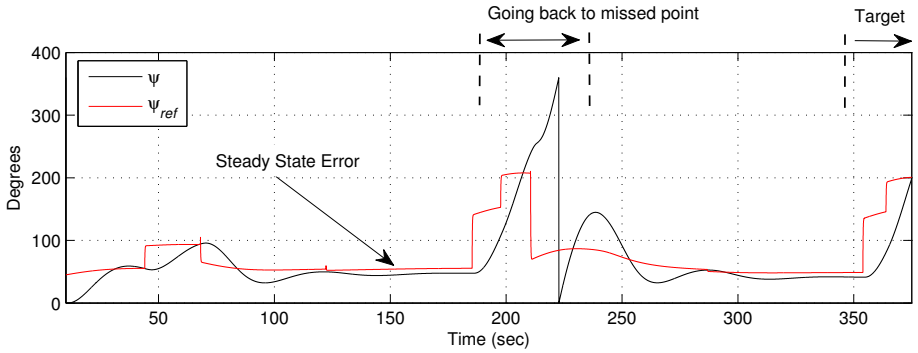

Fig. 8 Simulation-1, Heading Reference and Heading Signals

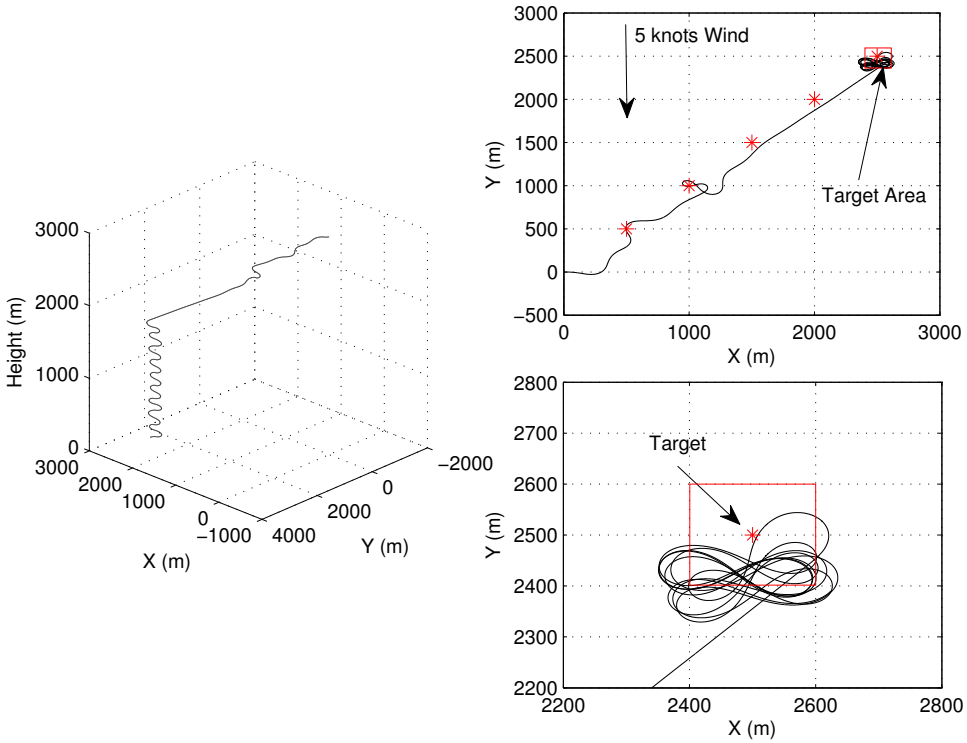

Fig. 9 Simulation-2, Proportional Control Only

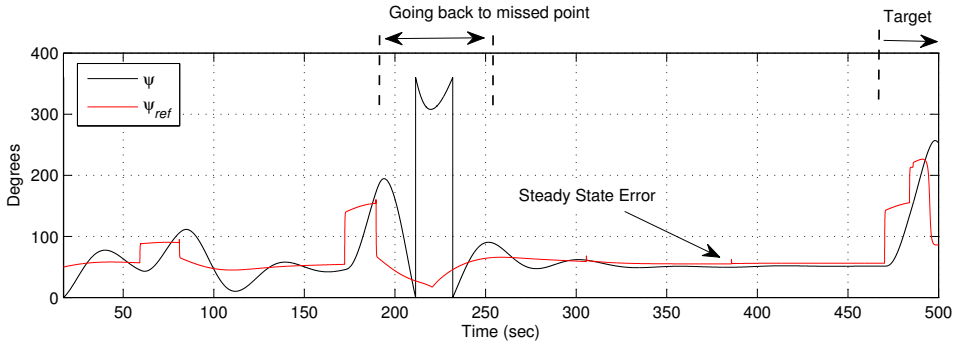

Fig. 10 Simulation-2, Heading Reference and Heading Signals

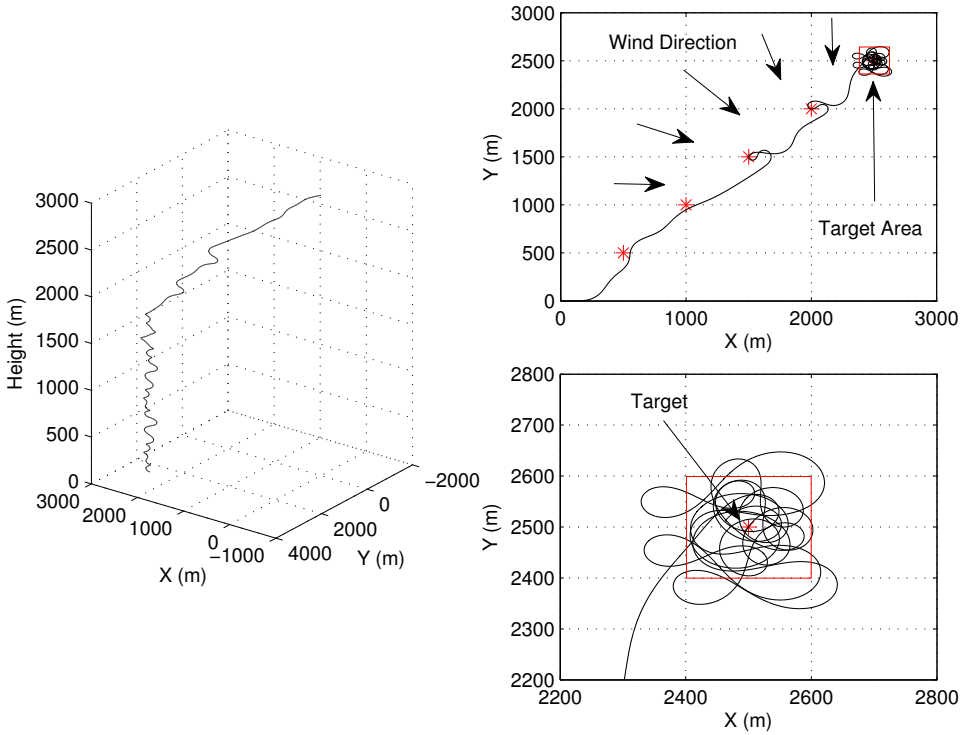

Fig. 11 Simulation-3, Proportional Controller Under Varying Wind Direction

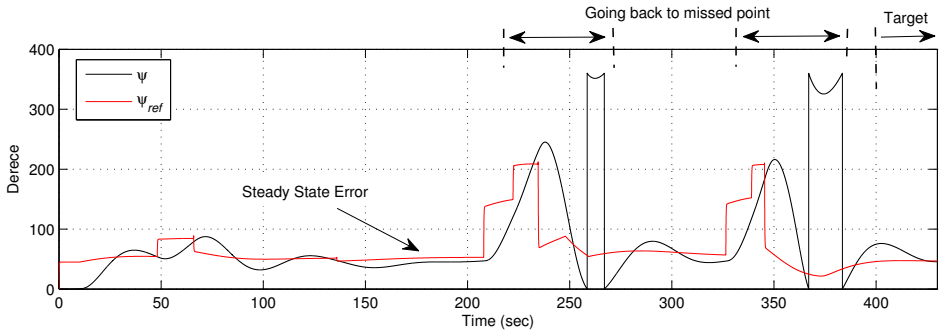

Fig. 12 Simulation-3, Heading Reference and Heading Signals

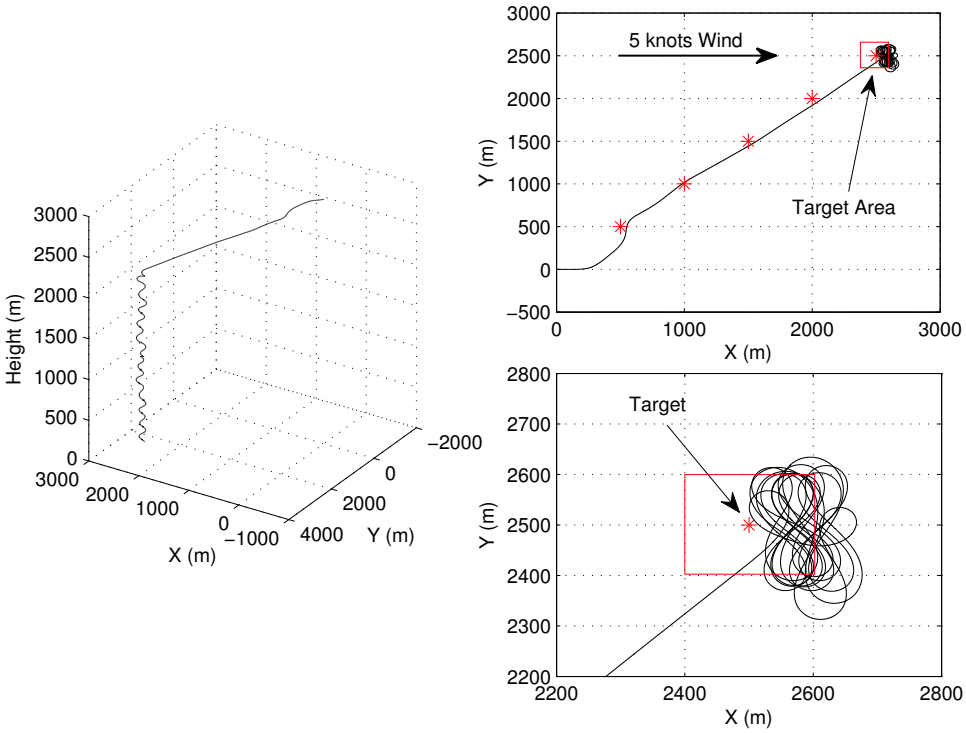

Fig. 13 Simulation-1, PID Controller

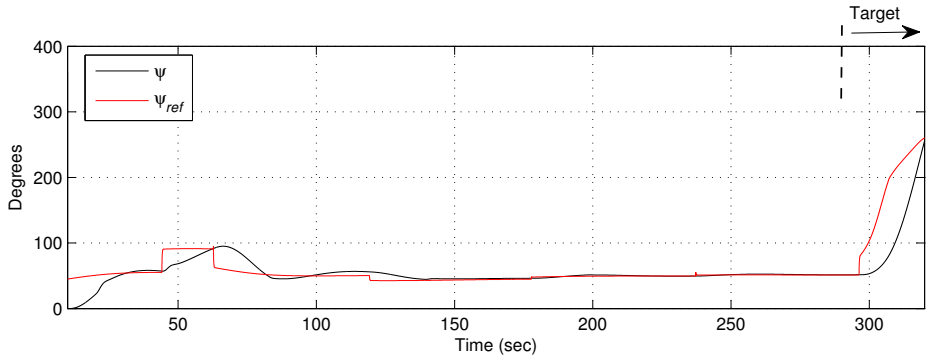

Fig. 14 Simulation-1, Heading Reference and Heading Signals, using PID Controller

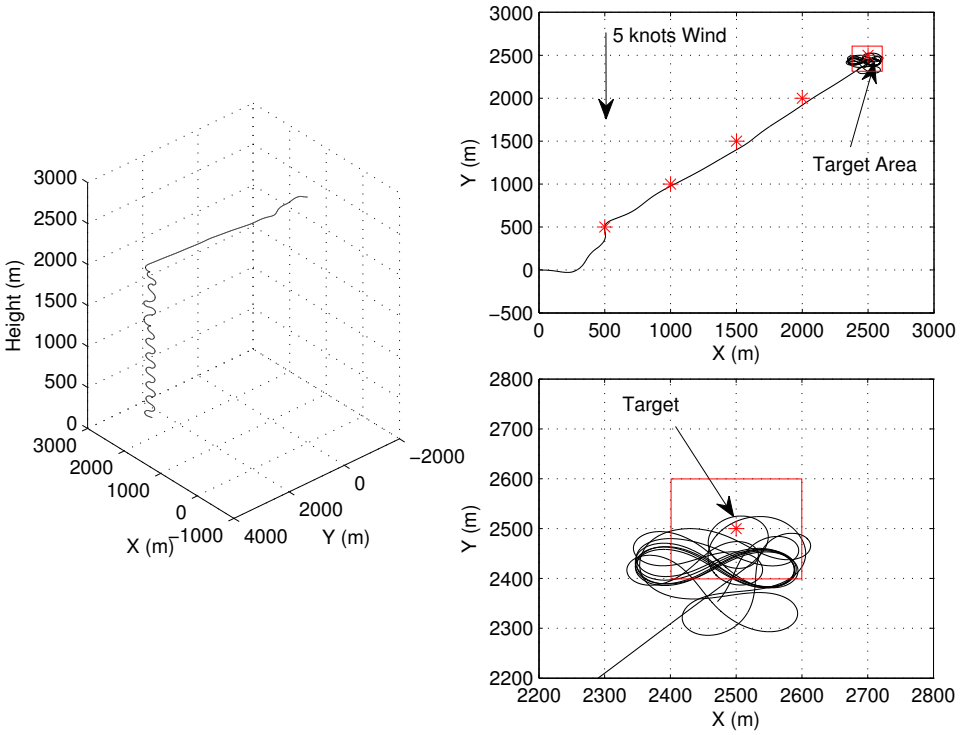

Fig. 15 Simulation-2, with PID Controller

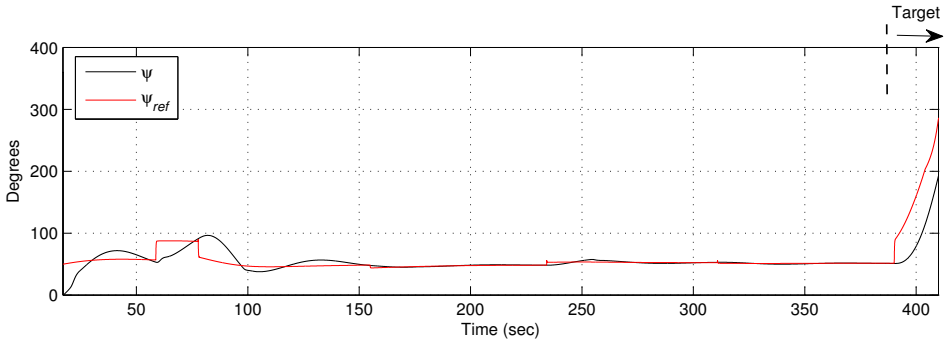

Fig. 16 Simulation-2, Heading Reference and Heading Signals, using PID Controller

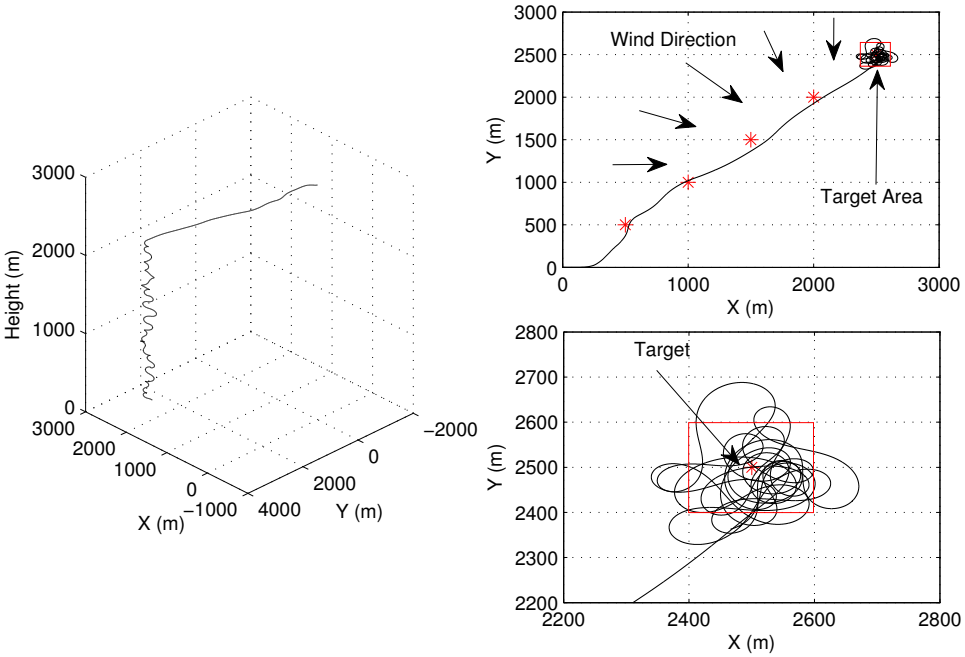

Fig. 17 Simulation-3, PID Controller Under Varying Wind Direction

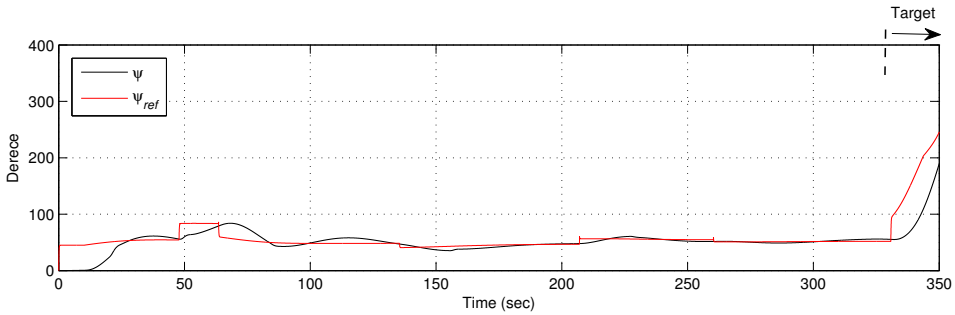

Fig. 18 Simulation-3, Heading Reference and Heading Signals, using PID Controller

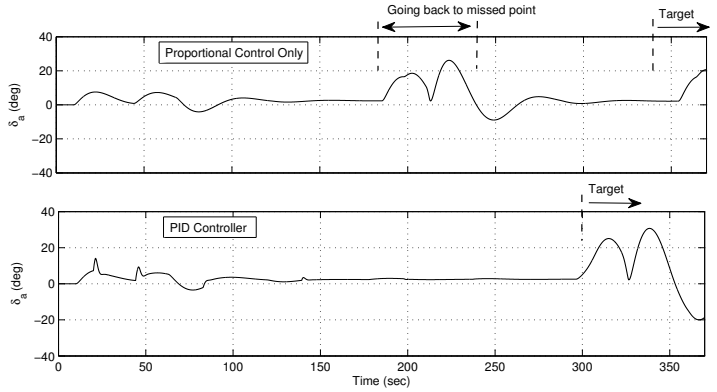

Fig. 19 Simulation-1, Comparison of Control Surface Deflections

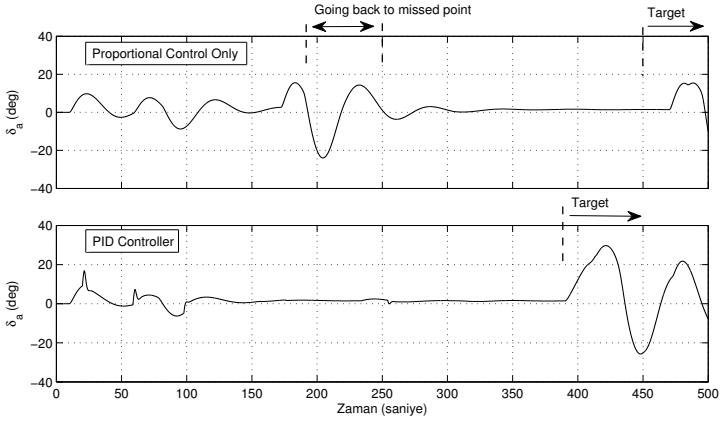

Fig. 20 Simulation-2, Comparison of Control Surface Deflections

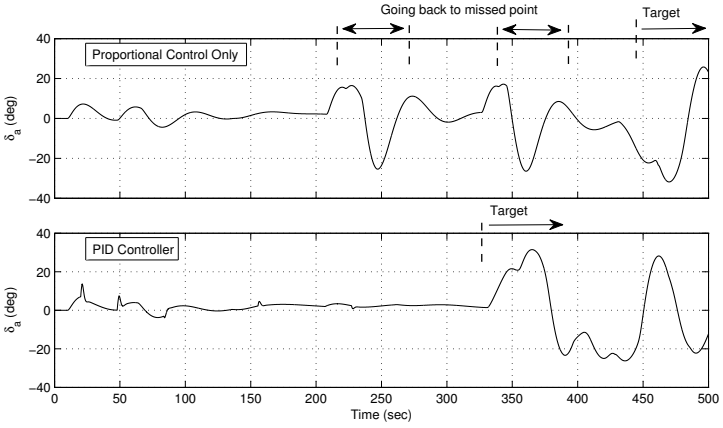

Fig. 21 Simulation-3, Comparison of Control Surface Deflections

5 Conclusion

This paper describes the development of a waypoint tracking control algorithm for a parachute-payload system. The introduced algorithm employs a waypoint navigation for a target approach. Simulation results for constant and varying wind conditions are presented and illustrated. The proposed control algorithm is capable of driving the system to the desired waypoints. It is concluded that with a proper use of the waypoint update criteria the system can be driven to the desired waypoints even when the inner loop controller does not perform well. The effectiveness of the control algorithm is also illustrated for the cases of wind presence, and when the heading controller is designed as a simple proportional gain.

References

1. Jann T., Advanced Features for Autonomous Parafoil Guidance, Navigation and Control, 18th AIAA Aerodynamic Decelerator Systems Technology Conference and Seminar, 2005.
2. Rademacher B. J. et al., Trajectory Design, Guidance and Control for Autonomous Parafoils, AIAA Guidance, Navigation and Control Conference and Exhibit, Honolulu, Hawaii, 18 - 21 August 2008.
3. Kaminer I.I., Yakimenko O. A., On the Development of GNC Algorithm for a High-Glide Payload Delivery System, Proceedings of 42nd IEEE Conference on Decision and Control, Maui, Hawaii, USA, Vol. 5, December 2003.
4. Calise A. J. et al., Modeling for Guidance and Control Design of Autonomous Guided Parafoils, 19th AIAA Aerodynamic Decelerator Systems Technology Conference and Seminar, Williamsburg, VA, 21 - 24 May 2007.
5. Slegers N., Costello M., Model Predictive Control of a Parafoil and Payload System, Journal of Guidance, Control, and Dynamics, Vol. 28, No. 4, July-August 2005.
6. Pollini L., Giulietti F., Innocenti M., Modeling, Simulation and Control of a Wing Parafoil for Atmosphere to Ground Flight, AIAA Modeling and Simulation Technologies Conference and Exhibit, Monterey, California, 5-8 August 2002.
7. Xie Z. et al., SDRE and Series Approximations Model Predictive Control for a Parafoil System, 2011 International Conference on Electric Information and Control Engineering (ICEICE), China, 15-17 April 2011.
8. Toglia C., Vendittelli M., Modeling and Motion Analysis of Autonomous Paragliders, No 2010-05, DIS Technical Reports, Department of Computer, Control and Management Engineering, Sapienza University of Rome, 2010.
9. Prakash O., Ananthkrishnan N., Modeling and Simulation of 9-DOF Parafoil-Payload System Flight Dynamics, AIAA Atmospheric Flight Mechanics Conference and Exhibit, Keystone, Colorado, August 2006.
10. Slegers N., Costello M., Aspects of Control for a Parafoil and Payload System, Journal of Guidance, Control, and Dynamics, Vol. 26, No. 6, November-December 2003.
11. Muller S., Wagner O., Sachs G., A High-fidelity Nonlinear Multibody Simulation Model for Parafoil Systems, 17th AIAA Aerodynamic Decelerator Systems Technology Conference and Seminar, May 2003.